

Strangelet search in Au+Au collisions at $\sqrt{s_{NN}} = 200$ GeV

B. I. Abelev,⁹ M. M. Aggarwal,³⁰ Z. Ahammed,⁴⁵ B. D. Anderson,²⁰ D. Arkhipkin,¹³ G. S. Averichev,¹² Y. Bai,²⁸ J. Balewski,¹⁷ O. Barannikova,⁹ L. S. Barnby,² J. Baudot,¹⁸ S. Baumgart,⁵⁰ V. V. Belaga,¹² A. Bellingeri-Laurikainen,⁴⁰ R. Bellwied,⁴⁸ F. Benedosso,²⁸ R. R. Betts,⁹ S. Bhardwaj,³⁵ A. Bhasin,¹⁹ A. K. Bhati,³⁰ H. Bichsel,⁴⁷ J. Bielcik,⁵⁰ J. Bielcikova,⁵⁰ L. C. Bland,³ S.-L. Blyth,²² M. Bombara,² B. E. Bonner,³⁶ M. Botje,²⁸ J. Bouchet,⁴⁰ A. V. Brandin,⁵² A. Bravar,³ T. P. Burton,² M. Bystersky,¹¹ R. V. Cadman,¹ X. Z. Cai,³⁹ H. Caines,⁵⁰ M. Calderón de la Barca Sánchez,⁶ J. Callner,⁹ O. Catu,⁵⁰ D. Cebra,⁶ Z. Chajecki,²⁹ P. Chaloupka,¹¹ S. Chattopadhyay,⁴⁵ H. F. Chen,³⁸ J. H. Chen,³⁹ J. Y. Chen,⁴⁹ J. Cheng,⁴³ M. Cherney,¹⁰ A. Chikanian,⁵⁰ W. Christie,³ S. U. Chung,³ J. P. Coffin,¹⁸ T. M. Cormier,⁴⁸ M. R. Cosentino,³⁷ J. G. Cramer,⁴⁷ H. J. Crawford,⁵ D. Das,⁴⁵ S. Dash,¹⁵ M. Daugherty,⁴² M. M. de Moura,³⁷ T. G. Dedovich,¹² M. DePhillips,³ A. A. Derevschikov,³² L. Didenko,³ T. Dietel,¹⁴ P. Djawotho,¹⁷ S. M. Dogra,¹⁹ X. Dong,²² J. L. Drachenberg,⁴¹ J. E. Draper,⁶ F. Du,⁵⁰ V. B. Dunin,¹² J. C. Dunlop,³ M. R. Dutta Mazumdar,⁴⁵ V. Eckardt,²⁴ W. R. Edwards,²² L. G. Efimov,¹² V. Emelianov,⁵² J. Engelage,⁵ G. Eppley,³⁶ B. Erasmus,⁴⁰ M. Estienne,¹⁸ P. Fachini,³ R. Fatemi,²³ J. Fedorisin,¹² A. Feng,⁴⁹ P. Filip,¹³ E. Finch,⁵⁰ V. Fine,³ Y. Fisyak,³ J. Fu,⁴⁹ C. A. Gagliardi,⁴¹ L. Gaillard,² M. S. Ganti,⁴⁵ E. Garcia-Solis,⁹ V. Ghazikhanian,⁷ P. Ghosh,⁴⁵ Y. G. Gorbunov,¹⁰ H. Gos,⁴⁶ O. Grebenyuk,²⁸ D. Grosnick,⁴⁴ S. M. Guertin,⁷ K. S. F. F. Guimaraes,³⁷ N. Gupta,¹⁹ B. Haag,⁶ T. J. Hallman,³ A. Hamed,⁴¹ J. W. Harris,⁵⁰ W. He,¹⁷ M. Heinz,⁵⁰ T. W. Henry,⁴¹ S. Heppelmann,³¹ B. Hippolyte,¹⁸ A. Hirsch,³³ E. Hjort,²² A. M. Hoffman,²³ G. W. Hoffmann,⁴² D. Hofman,⁹ R. Hollis,⁹ M. J. Horner,²² H. Z. Huang,⁷ E. W. Hughes,⁴ T. J. Humanic,²⁹ G. Igo,⁷ A. Iordanova,⁹ P. Jacobs,²² W. W. Jacobs,¹⁷ P. Jakl,¹¹ F. Jia,²¹ P. G. Jones,² E. G. Judd,⁵ S. Kabana,⁴⁰ K. Kang,⁴³ J. Kapitan,¹¹ M. Kaplan,⁸ D. Keane,²⁰ A. Kechechyan,¹² D. Kettler,⁴⁷ V. Yu. Khodyrev,³² B. C. Kim,³⁴ J. Kirelyuk,²² A. Kisiel,⁴⁶ E. M. Kislov,¹² S. R. Klein,²² A. G. Knospe,⁵⁰ A. Kocoloski,²³ D. D. Koetke,⁴⁴ T. Kollegger,¹⁴ M. Kopytine,²⁰ L. Kotchenda,⁵² V. Kouchpil,¹¹ K. L. Kowalik,²² P. Kravtsov,⁵² V. I. Kravtsov,³² K. Krueger,¹ C. Kuhn,¹⁸ A. I. Kulikov,¹² A. Kumar,³⁰ P. Kurnadi,⁷ A. A. Kuznetsov,¹² M. A. C. Lamont,⁵⁰ J. M. Landgraf,³ S. Lange,¹⁴ S. LaPointe,⁴⁸ F. Laue,³ J. Lauret,³ A. Lebedev,³ R. Lednicky,¹³ C.-H. Lee,³⁴ S. Lehecka,¹² M. J. LeVine,³ C. Li,³⁸ Q. Li,⁴⁸ Y. Li,⁴³ G. Lin,⁵⁰ X. Lin,⁴⁹ S. J. Lindenbaum,²⁷ M. A. Lisa,²⁹ F. Liu,⁴⁹ H. Liu,³⁸ J. Liu,³⁶ L. Liu,⁴⁹ T. Ljubicic,³ W. J. Llope,³⁶ R. S. Longacre,³ W. A. Love,³ Y. Lu,⁴⁹ T. Ludlam,³ D. Lynn,³ G. L. Ma,³⁹ J. G. Ma,⁷ Y. G. Ma,³⁹ D. P. Mahapatra,¹⁵ R. Majka,⁵⁰ L. K. Mangotra,¹⁹ R. Manweiler,⁴⁴ S. Margetis,²⁰ C. Markert,⁴² L. Martin,⁴⁰ H. S. Matis,²² Yu. A. Matulenko,³² C. J. McClain,¹ T. S. McShane,¹⁰ Yu. Melnick,³² A. Meschanin,³² J. Millane,²³ M. L. Miller,²³ N. G. Minaev,³² S. Mioduszewski,⁴¹ C. Mironov,²⁰ A. Mischke,²⁸ J. Mitchell,³⁶ B. Mohanty,²² D. A. Morozov,³² M. G. Munhoz,³⁷ B. K. Nandi,¹⁶ C. Nattrass,⁵⁰ T. K. Nayak,⁴⁵ J. M. Nelson,² N. S. Nepali,²⁰ P. K. Netrakanti,³³ L. V. Nogach,³² S. B. Nurushev,³² G. Odyniec,²² A. Ogawa,³ V. Okorokov,⁵² M. Oldenbourg,²² D. Olson,²² M. Pachr,¹¹ S. K. Pal,⁴⁵ Y. Panebratsev,¹² A. I. Pavlinov,⁴⁸ T. Pawlak,⁴⁶ T. Peitzmann,²⁸ V. Perevoztchikov,³ C. Perkins,⁵ W. Peryt,⁴⁶ S. C. Phatak,¹⁵ M. Planinic,⁵¹ J. Pluta,⁴⁶ N. Poljak,⁵¹ N. Porile,³³ A. M. Poskanzer,²² M. Potekhin,³ E. Potrebenikova,¹² B. V. K. S. Potukuchi,¹⁹ D. Prindle,⁴⁷ C. Pruneau,⁴⁸ J. Putschke,²² I. A. Qattan,¹⁷ R. Raniwala,³⁵ S. Raniwala,³⁵ R. L. Ray,⁴² D. Relyea,⁴ A. Ridiger,⁵² H. G. Ritter,²² J. B. Roberts,³⁶ O. V. Rogachevskiy,¹² J. L. Romero,⁶ A. Rose,²² C. Roy,⁴⁰ L. Ruan,²² M. J. Russcher,²⁸ R. Sahoo,¹⁵ I. Sakrejda,²² T. Sakuma,²³ S. Salur,⁵⁰ J. Sandweiss,⁵⁰ M. Sarsour,⁴¹ P. S. Sazhin,¹² J. Schambach,⁴² R. P. Scharenberg,³³ N. Schmitz,²⁴ J. Seger,¹⁰ I. Selyuzhenkov,⁴⁸ P. Seyboth,²⁴ A. Shabetai,¹⁸ E. Shalahiev,¹² M. Shao,³⁸ M. Sharma,³⁰ W. Q. Shen,³⁹ S. S. Shimanskiy,¹² E. P. Sichtermann,²² F. Simon,²³ R. N. Singaraju,⁴⁵ N. Smirnov,⁵⁰ R. Snellings,²⁸ P. Sorensen,³ J. Sowinski,¹⁷ J. Speltz,¹⁸ H. M. Spinka,¹ B. Srivastava,³³ A. Stadnik,¹² T. D. S. Stanislaus,⁴⁴ D. Staszak,⁷ R. Stock,¹⁴ M. Strikhanov,⁵² B. Stringfellow,³³ A. A. P. Suaide,³⁷ M. C. Suarez,⁹ N. L. Subba,²⁰ M. Sumner,¹¹ X. M. Sun,²² Z. Sun,²¹ B. Surrow,²³ T. J. M. Symons,²² A. Szanto de Toledo,³⁷ B. Szeliga,⁴⁸ J. Takahashi,³⁷ A. H. Tang,³ T. Tarnowsky,³³ J. H. Thomas,²² A. R. Timmins,² S. Timoshenko,⁵² M. Tokarev,¹² T. A. Trainor,⁴⁷ S. Trentalange,⁷ R. E. Tribble,⁴¹ O. D. Tsai,⁷ J. Ulery,³³ T. Ullrich,³ D. G. Underwood,¹ G. Van Buren,³ N. van der Kolk,²⁸ M. van Leeuwen,²² A. M. Vander Molen,²⁵ R. Varma,¹⁶ I. M. Vasilevski,¹³ A. N. Vasiliev,³² R. Vernet,¹⁸ S. E. Vigdor,¹⁷ Y. P. Viyogi,¹⁵ S. Vokal,¹² S. A. Voloshin,⁴⁸ W. T. Waggoner,¹⁰ F. Wang,³³ G. Wang,⁷ J. S. Wang,²¹ X. L. Wang,³⁸ Y. Wang,⁴³ J. W. Watson,²⁰ J. C. Webb,⁴⁴ G. D. Westfall,²⁵ A. Wetzler,²² C. Whitten Jr.,⁷ H. Wieman,²² S. W. Wissink,¹⁷ R. Witt,⁵⁰ J. Wu,³⁸ Y. Wu,⁴⁹ N. Xu,²² Q. H. Xu,²² Z. Xu,³ P. Yepes,³⁶ I.-K. Yoo,³⁴ Q. Yue,⁴³ V. I. Yurevich,¹² W. Zhan,²¹ H. Zhang,³ W. M. Zhang,²⁰ Y. Zhang,³⁸ Z. P. Zhang,³⁸ Y. Zhao,³⁸ C. Zhong,³⁹ J. Zhou,³⁶ R. Zoulkarneev,¹³ Y. Zoulkarneeva,¹³ A. N. Zubarev,¹² and J. X. Zuo³⁹

(STAR Collaboration)

¹Argonne National Laboratory, Argonne, Illinois 60439, USA²University of Birmingham, Birmingham, United Kingdom³Brookhaven National Laboratory, Upton, New York 11973, USA⁴California Institute of Technology, Pasadena, California 91125, USA⁵University of California, Berkeley, California 94720, USA⁶University of California, Davis, California 95616, USA⁷University of California, Los Angeles, California 90095, USA⁸Carnegie Mellon University, Pittsburgh, Pennsylvania 15213, USA⁹University of Illinois, Chicago, Illinois, USA¹⁰Creighton University, Omaha, Nebraska 68178, USA

- ¹¹*Nuclear Physics Institute AS CR, 250 68 Řež/Prague, Czech Republic*
¹²*Laboratory for High Energy (JINR), Dubna, Russia*
¹³*Particle Physics Laboratory (JINR), Dubna, Russia*
¹⁴*University of Frankfurt, Frankfurt, Germany*
¹⁵*Institute of Physics, Bhubaneswar 751005, India*
¹⁶*Indian Institute of Technology, Mumbai, India*
¹⁷*Indiana University, Bloomington, Indiana 47408, USA*
¹⁸*Institut de Recherches Subatomiques, Strasbourg, France*
¹⁹*University of Jammu, Jammu 180001, India*
²⁰*Kent State University, Kent, Ohio 44242, USA*
²¹*Institute of Modern Physics, Lanzhou, People's Republic of China*
²²*Lawrence Berkeley National Laboratory, Berkeley, California 94720, USA*
²³*Massachusetts Institute of Technology, Cambridge, Massachusetts 02139-4307, USA*
²⁴*Max-Planck-Institut für Physik, Munich, Germany*
²⁵*Michigan State University, East Lansing, Michigan 48824, USA*
²⁶*Moscow Engineering Physics Institute, Moscow, Russia*
²⁷*City College of New York, New York City, New York 10031, USA*
²⁸*NIKHEF and Utrecht University, Amsterdam, The Netherlands*
²⁹*Ohio State University, Columbus, Ohio 43210, USA*
³⁰*Panjab University, Chandigarh 160014, India*
³¹*Pennsylvania State University, University Park, Pennsylvania 16802, USA*
³²*Institute of High Energy Physics, Protvino, Russia*
³³*Purdue University, West Lafayette, Indiana 47907, USA*
³⁴*Pusan National University, Pusan, Republic of Korea*
³⁵*University of Rajasthan, Jaipur 302004, India*
³⁶*Rice University, Houston, Texas 77251, USA*
³⁷*Universidade de Sao Paulo, Sao Paulo, Brazil*
³⁸*University of Science & Technology of China, Hefei 230026, People's Republic of China*
³⁹*Shanghai Institute of Applied Physics, Shanghai 201800, People's Republic of China*
⁴⁰*SUBATECH, Nantes, France*
⁴¹*Texas A&M University, College Station, Texas 77843, USA*
⁴²*University of Texas, Austin, Texas 78712, USA*
⁴³*Tsinghua University, Beijing 100084, People's Republic of China*
⁴⁴*Valparaiso University, Valparaiso, Indiana 46383, USA*
⁴⁵*Variable Energy Cyclotron Centre, Kolkata 700064, India*
⁴⁶*Warsaw University of Technology, Warsaw, Poland*
⁴⁷*University of Washington, Seattle, Washington 98195, USA*
⁴⁸*Wayne State University, Detroit, Michigan 48201, USA*
⁴⁹*Institute of Particle Physics, CCNU (HZNU), Wuhan 430079, People's Republic of China*
⁵⁰*Yale University, New Haven, Connecticut 06520, USA*
⁵¹*University of Zagreb, Zagreb, HR-10002, Croatia*
⁵²*Moscow Engineering Physics Institute, Moscow, Russia*

(Received 27 November 2005; revised manuscript received 21 January 2007; published 25 July 2007)

We have searched for strangelets in a triggered sample of 61 million central (top 4%) Au+Au collisions at $\sqrt{s_{NN}} = 200$ GeV near beam rapidities at the STAR solenoidal tracker detector at the BNL Relativistic Heavy Ion Collider. We have sensitivity to metastable strangelets with lifetimes of order ≥ 0.1 ns, in contrast to limits over ten times longer in BNL Alternating Gradient Synchrotron (AGS) studies and longer still at the CERN Super Proton Synchrotron (SPS). Upper limits of a few 10^{-6} to 10^{-7} per central Au+Au collision are set for strangelets with mass ≥ 30 GeV/c².

DOI: [10.1103/PhysRevC.76.011901](https://doi.org/10.1103/PhysRevC.76.011901)

PACS number(s): 25.75.Dw

Strange quark matter (SQM) is a hypothetical state of matter consisting of roughly equal numbers of u , d , and s quarks. It might have lower energy per baryon than ordinary nuclear matter and thus might be the true ground state of baryonic matter [1,2]. Strangelets might be stable, or metastable with

a weak-decay lifetime. They are predicted to have a small or zero charge-to-mass ratio and could carry either sign of charge. SQM has been proposed to explain several astrophysical phenomena [2,3], to be used as a clean energy source [4], to be a QCD laboratory [5], and to cause possible exotic scenarios [6].

Terrestrial materials [7], cosmic remnants [7], and heavy ion collisions (studied by E864 and E896 at BNL and NA52 at CERN) [8,9] have been searched for strangelets. All of these searches yielded negative results and reported complementary upper limits.

Coalescence [10] and thermal statistical [11] models predict low rates of strangelet production at midrapidity, as supported by related measurements of nucleon coalescence [12]. If a quark-gluon plasma (QGP) is created in heavy ion collisions, it could cool down by distillation (kaon emission) and condense to strange-quark-rich matter in its ground state—a strangelet [13,14]. However, this requires a net baryon excess and a nonexplosive process in the collisions [13,15], neither of which is favored at midrapidity at the BNL Relativistic Heavy Ion Collider (RHIC) [16].

Pomerons—force carriers invoked in some soft-interaction descriptions—have been introduced as a possible mechanism for strangelet production near spectator rapidities; QGP formation is not required [17]. Models based on color superconductivity predict that quark pairs at high baryon density have lower energy when colors and flavors are correlated to form color-flavor locked (CFL) pairs [18]; positively charged strangelets are favored because of the surface depletion of s quarks [18]. In such states, u and d outnumber s quarks. These scenarios require high baryon density and favor forward rapidities, hence the focus of the present search. We investigate the energy and shower profiles in calorimeters at zero degrees relative to the beamlines. This approach provides excellent sensitivity for short-lived strangelets and has a near uniform acceptance for strangelets with a wide range of charge to mass ratios, including neutrals. It complements most past experiments, which searched for strangelets with the hope that most of the strangelets are produced around midrapidity [9].

A strangelet produced in the forward region at RHIC will have a small charge-to-mass ratio, and its rigidity (momentum/ Z , where Z is the particle's charge in multiples of the electron charge) will be exceptionally large. Thus it will follow a nearly straight trajectory and deposit a large signal in one of the zero degree calorimeters (ZDCs) [19], which are located just beyond the nearest beam dipole magnets (DX) to the experiment. Normal spectator fragments other than neutrons cannot reach the ZDCs due to the strong fields of the DX magnets. There is one ZDC to the east of the interaction region at STAR, and another to the west, located 18 m from the center of the detector. The analog to digital converter (ADC) gate for the ZDCs is open from -15 to $+70$ ns relative to the arrival time for particles from the interaction moving at the speed of light. The acceptance for a charged strangelet in a ZDC depends on its rigidity and, because of the ZDC's rectangular shape, depends slightly on its azimuthal angle. The left panel of Fig. 1 shows the acceptance in total rigidity and transverse rigidity. The acceptance for a neutral strangelet depends on its pseudorapidity η ($\equiv -\ln \tan(\theta/2)$, where $\cos \theta = p_z/p$) and azimuthal angle ϕ (Fig. 1, right panel).

A strangelet would produce a large shower in a ZDC, comparable to the signal from a cluster of spectator neutrons. The latter signal is dispersed in the transverse plane, since transverse momentum for spectator neutrons is comparable to Fermi momentum. In contrast, the shower from a strangelet

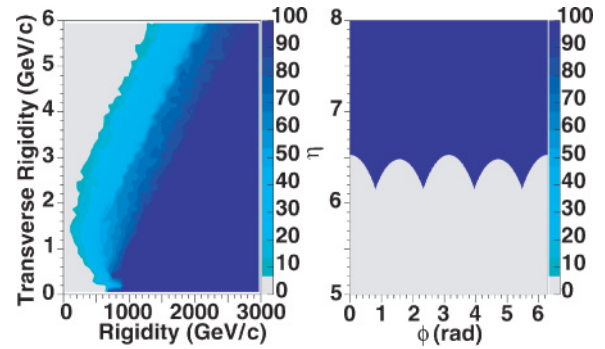


FIG. 1. (Color online) Geometrical acceptance indicated by color coding (in %) for the STAR ZDC-SMD as a function of transverse rigidity and rigidity for charged strangelets (left), and as a function of pseudorapidity η and azimuthal angle ϕ for neutral strangelets (right).

would originate at a single point in the ZDC, as illustrated by the GEANT simulation in Fig. 2, where the shower profile in the X-Y (transverse) plane is plotted for spectator neutrons (left) and strangelets (right). In this simulation, each neutron cluster consists of 35 neutrons with a maximum p_t of 270 MeV/c, and each strangelet has the same mass as 35 neutrons, with the assumed cross section being the same as that of a neutron times the baryon number of the strangelet. The rms of the radial extent of the strangelet shower is $(69 \pm 12)\%$ times the rms from the simulated 35-neutron spectator remnant. A change in the assumed mass of the strangelet or in the number of spectator neutrons does not affect this ratio. For the scenario of a strangelet accompanied by neutrons, the mean square is a linear combination of that from strangelet and neutrons. When a strangelet is accompanied by ten neutrons, the ratio increases by 12%. Therefore, the strangelet signature used in this ZDC search is a large energy deposition with a narrow transverse shower profile in central Au+Au collisions.

Each ZDC incorporates a shower maximum detector (SMD) [20] with seven vertical and eight horizontal slats, providing event-by-event information that allows a strangelet signal to be distinguished from multiple neutrons via the narrower lateral extent of its shower. The strangelet trigger takes advantage of the anticorrelation of particle multiplicity and ZDC signal for central heavy ion collisions; in central events, the background ZDC signal from spectator neutrons is small, and the probability of production of an exotic high-mass object is highest. We take the shower profile of neutrons from peripheral events as a reference sample because of the large

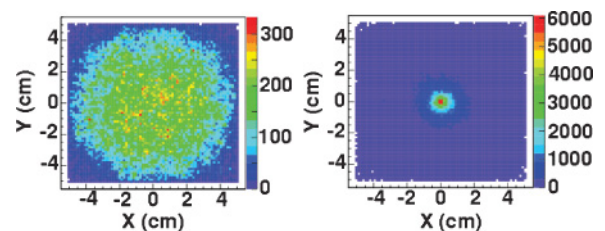


FIG. 2. (Color online) Shower profile of neutron clusters (left) and strangelets (right) from simulations.

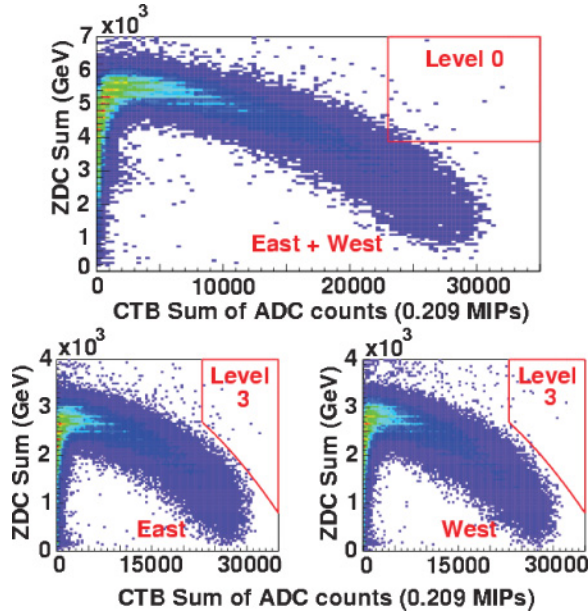


FIG. 3. (Color online) Level 0 and Level 3 triggers.

ZDC signals they produce. The particle multiplicity used for online triggers in STAR is measured primarily with the central trigger barrel (CTB) covering $|\eta| < 1$ and $0 < \phi < 2\pi$ [21]. Although a normal central event produces a small signal in the ZDC, a peripheral Au+Au collision can accompany the central event in one bunch crossing and may result in a background event with a large ZDC signal. These background double-interaction events happen at a level of 0.1–0.01% with current luminosity ($1 \times 10^{27} \text{ cm}^{-2} \text{ s}^{-1}$). The ZDC-SMD provides the needed shower profile information to distinguish those events from strangelet events.

During the 2004 run, two special triggers for the strangelet search were implemented. The trigger conditions at level zero (L0) are that the signal from the CTB exceeds 23000 ADC counts (approximately 4800 minimum ionizing particles), which corresponds to selecting the top 4% most central events, and the signal sum from both ZDCs exceeds 3875 GeV (39 neutron equivalents); see Fig. 3, upper panel. The total rejection obtained with this trigger is 99.25%.

In total, we recorded 458000 L0 triggered events, sampling 61 million 4% most central Au+Au events during the 2004 run. A level-three (L3) trigger was implemented to write to an express stream approximately 20% of the events that passed the L0 trigger. The L3 trigger required that the correlation between either one of the ZDCs and the CTB signal must lie above the curve made by the correlation observed in minimum-bias events (Fig. 3, bottom panels). Our analysis only applies to events that pass the L3 trigger. Additional offline requirements are that the event vertex z position as determined from the ZDCs was within 2σ of the z position determined from Time Projection Chamber (TPC) tracking, and the energy sum measured in the SMDs was within 2σ of the energy sum measured in the ZDCs. The first requirement removes possible events from pileup, and the second ensures that large signals are deposited in the ZDCs and their associated SMDs for triggered events. Finally, since we record the ADC

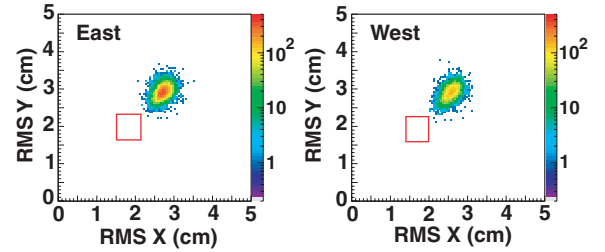


FIG. 4. (Color online) Distribution of rms from east and west SMDs.

value for each ZDC module, as well as the ADC value of the analog sum of the three ZDC modules, we can compare these two signals to eliminate any events with an electronics-related inconsistency. Events that pass all triggers and cuts have a typical energy deposition of 3300 GeV at the ZDC selected by the L3 trigger.

We recorded the signal of each SMD slat for each event and computed the signal-weighted centroid and variance for each event in both the X and Y directions. Figure 4 shows the distribution of rms values from the SMD in the X - Y plane for strangelet candidates surviving the cuts described previously. If a strangelet is created in the collision and reaches one of the ZDC-SMDs, it is expected to produce a large signal with a relatively narrow shower profile in the SMD. Any candidate with such characteristics would show up in the lower-left boxes in one of the two panels. The position and size of the two boxes are obtained from the simulation. If a different reference sample other than peripheral events is used to study the possible mismatch of shower profile, the position and width of the search windows change by only about 3%. Figure 4 shows that the rms distributions for both SMDs from the strangelet candidates are well above the shower profiles expected from strangelets. We conclude that no candidate with anomalously low rms in both X and Y directions is observed.

To establish an upper limit for strangelet production, we assume a source distribution having an inverse slope in transverse mass of 160 MeV, which is a typical chemical freeze-out temperature at RHIC. Since strangelet production could be enhanced at midrapidity because of the formation of a QGP [13], or enhanced at forward rapidity due to the Pomeron-cutting mechanism [17], we assume a flat distribution in rapidity up to beam rapidity. Correcting for our trigger efficiencies and timing gate efficiencies, as well as our acceptance, we present our upper limit at 90% confidence level as a function of mass in Fig. 5.

The upper limits decrease as the assumed strangelet mass increases. The limits are 6.9×10^{-6} and 4.5×10^{-7} per central Au+Au collision for neutral strangelets with mass 30 and 100 GeV/ c^2 , respectively. Limits for charged strangelets are different because of the magnets in front of the ZDC-SMDs. Varying the assumed transverse mass slope for strangelets by ± 60 MeV results in little change to the upper limits. However, the limits depend strongly on the rapidity distribution. For the strangelet mass range presented here, our acceptance decreases dramatically at $y \gtrsim 4$ with the detailed geometric acceptance shown in Fig. 1. This dependence is not uncommon, because none of the strangelet search experiments have 4π coverage

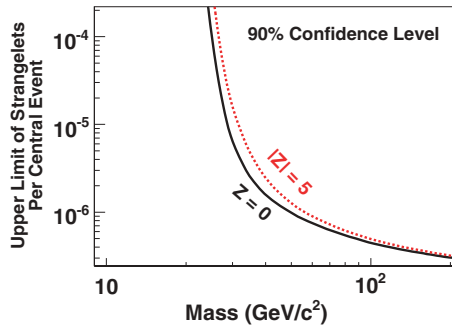


FIG. 5. (Color online) Upper limit, with 90% confidence level, of strangelet production as a function of mass, for neutral strangelets (solid line) and strangelets with charge = 5 (dashed line). Limits for strangelets with charge 1–4 lie between the two lines.

over all the kinematics while the limits are for production per interaction in all kinematics. Although our upper limits are roughly comparable to those set by other heavy ion experiments (ranging from 10^{-7} to 10^{-9} , as shown in Fig. 6 and Ref. [9]), it is difficult to compare precisely the limits with previous experiments due to the difference in collision centrality selection, acceptance, production model, rapidity search window, and beam energy. Unfortunately, the theoretically expected yield in the forward region has yet to be calculated.

In summary, the present search is the first one at RHIC energies in the forward region and has produced no candidates. The lifetime limits are less sensitive to experimental details than the limits in terms of production per event. Figure 6 shows that this search puts much more stringent limits (around 0.1 ns, more than an order of magnitude lower than before) on the lifetime of metastable strangelets. We emphasize that our search is generically sensitive to exotic objects with small charge-to-mass ratio in the kinematic regions shown in Fig. 1.

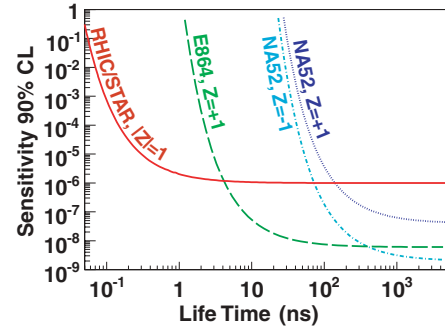


FIG. 6. (Color online) Upper limit of strangelet production at 90% confidence level as a function of lifetime for strangelet with mass $50 \text{ GeV}/c^2$, for which all experiments have a sensitivity. Solid, dashed, dot-dashed, and dotted lines are the limits of $|Z| = 1$ strangelets from the 4% most central Au+Au collisions at RHIC, $Z = +1$ strangelets from E864/AGS for the 10% most central Au+Pt collisions, and $Z = -1$ and $Z = +1$ strangelets from NA52/SPS for minimum-bias Pb+Pb collisions, respectively.

We thank Sebastian White for consultations and help in building the STAR ZDC-SMDs. We thank the RHIC Operations Group and RCF at BNL, and the NERSC Center at LBNL for their support. This work was supported in part by the Offices of NP and HEP within the U.S. DOE Office of Science; the U.S. NSF; the BMBF of Germany; CNRS/IN2P3, RA, RPL, and EMN of France; EPSRC of the United Kingdom; FAPESP of Brazil; the Russian Ministry of Science and Technology; the Ministry of Education and the NNSFC of China; IRP and GA of the Czech Republic; FOM of the Netherlands; DAE, DST, and CSIR of the Government of India; Swiss NSF; the Polish State Committee for Scientific Research; SRDA of Slovakia; and the Korea Sci. & Eng. Foundation.

- [1] A. R. Bodmer, Phys. Rev. D **4**, 1601 (1971).
- [2] E. Witten, Phys. Rev. D **30**, 272 (1984).
- [3] J. Madsen and J. M. Larsen, Phys. Rev. Lett. **90**, 121102 (2003); J. Madsen, *ibid.* **85**, 10 (2000).
- [4] G. L. Shaw, M. Shin, M. Desai, and R. H. Dalitz, Nature (London) **337**, 436 (1989).
- [5] E. Farhi and R. L. Jaffe, Phys. Rev. D **30**, 2379 (1984).
- [6] R. L. Jaffe, W. Busza, J. Sandweiss, and F. Wilczek, Rev. Mod. Phys. **72**, 1125 (2000).
- [7] R. Klingenberg, J. Phys. G **27**, 475 (2001); P. Mueller *et al.*, Phys. Rev. Lett. **92**, 022501 (2004); Z. T. Lu *et al.*, Nucl. Phys. A **754**, 361 (2005); for earlier searches, see R. Klingenberg, J. Phys. G **25**, R273 (1999).
- [8] H.-C. Liu and G. L. Shaw, Phys. Rev. D **30**, 1137 (1984).
- [9] R. Arsenescu *et al.*, New J. Phys. **4**, 96 (2002); R. Arsenescu *et al.*, J. Phys. G **27**, 487 (2001); T. A. Armstrong *et al.*, Phys. Rev. C **63**, 054903 (2001); H. Caines *et al.*, J. Phys. G **27**, 311 (2001); T. A. Armstrong *et al.*, Phys. Rev. Lett. **79**, 3612 (1997); G. Appelquist *et al.*, *ibid.* **76**, 3907 (1996); A. Rusek *et al.*, Phys. Rev. C **54**, R15 (1996); D. Beavis *et al.*, Phys. Rev. Lett. **75**, 3078 (1995); K. Borer *et al.*, *ibid.* **72**, 1415 (1994); M. Aoki *et al.*, *ibid.* **69**, 2345 (1992); J. Barrette *et al.*, Phys. Lett. B **252**, 550 (1990).
- [10] A. Baltz *et al.*, Phys. Lett. B **325**, 7 (1994).
- [11] P. Braun-Munzinger and J. Stachel, J. Phys. G **21**, L17 (1995).
- [12] T. A. Armstrong *et al.*, Phys. Rev. Lett. **83**, 5431 (1999); Phys. Rev. C **61**, 064908 (2000); **63**, 054903 (2001).
- [13] C. Greiner, P. Koch, and H. Stöcker, Phys. Rev. Lett. **58**, 1825 (1987); C. Greiner and H. Stöcker, Phys. Rev. D **44**, 3517 (1991).
- [14] H. J. Crawford, M. S. Desai, and G. L. Shaw, Phys. Rev. D **45**, 857 (1992).
- [15] J. Sandweiss, J. Phys. G **30**, S51 (2004).
- [16] J. Adams *et al.*, Nucl. Phys. A **757**, 102 (2005).
- [17] M. Bleicher *et al.*, Phys. Rev. Lett. **92**, 072301 (2004).
- [18] J. Madsen, Phys. Rev. Lett. **87**, 172003 (2001); **85**, 4687 (2000).
- [19] C. Adler, A. Denisov, E. Garcia, M. Murray, H. Ströbele, and S. White, Nucl. Instrum. Methods A **499**, 433 (2003); **470**, 488 (2001).
- [20] STAR ZDC-SMD proposal, STAR Note SN-0448, 2003 (unpublished).
- [21] F. S. Bieser *et al.*, Nucl. Instrum. Methods A **499**, 766 (2003).